Redox Modulation of Cyclic Electron Flow around Photosystem I in C3 Plants[†]

Cécile Breyton,[‡] Beena Nandha,[§] Giles N. Johnson,[§] Pierre Joliot,[||] and Giovanni Finazzi*,[||]

UMR-7099, CNRS-Université Paris-7, Institut de Biologie Physico-Chimique, Paris, France, Faculty of Life Sciences, University of Manchester, Manchester, U.K., and UMR-7141 CNRS-Université Paris-6, Institut de Biologie Physico-Chimique, Paris, France

Received July 17, 2006; Revised Manuscript Received September 5, 2006

ABSTRACT: We have investigated the occurrence of cyclic electron flow in intact spinach leaves. In particular, we have tested the hypothesis that cyclic flow requires the presence of supercomplexes in the thylakoid membrane or other strong associations between proteins. Using biochemical approaches, we found no evidence of the presence of supercomplexes related to cyclic electron flow, making previous structural explanations for the modulation of cyclic flow rather unlikely. On the other hand, we found that the fraction of photosystem I complexes engaged in cyclic flow could be modulated by changes in the redox state of the chloroplast stroma. Our findings support therefore a dynamic model for the occurrence of linear and cyclic electron flow in C3 plants, based on the competition between cytochrome b_6f and FNR for electrons carried by ferredoxin. This would be ultimately regulated by the balance between the redox state of PSI acceptors and donors during photosynthesis, in a diffusing system.

Photosynthesis involves the transfer of electrons from water to $NADP^+$ via two photosystems, the so-called linear path, forming NADPH. Electron transfer also results in proton translocation across the thylakoid membrane, generating a transmembrane pH gradient, which drives the synthesis of ATP. Both NADPH and ATP are then used for carbon fixation. Given that the H^+/ATP efficiency of this process is expected to be ∼4.7, linear electron transport alone is probably unable to generate the ATP/NADPH stoichiometry of 1.5 that is required for carbon fixation, as its maximum H^+/NADPH stoichiometry is 6 (see, for example, ref *1*). Alternative electron transport pathways are thus required to provide the "extra" ATP. Besides electron flow to oxygen [the Mehler reaction (*2*)] or to mitochondrial electron acceptors [the so-called "malate-shunt" (*3*)], cyclic electron flow around PSI was recently proposed to represent the most prominent candidate (*4*, *5*). Indeed, this pathway results in the generation of a proton gradient, leading to the production of ATP, but does not involve the net production of NADPH (*6*−*7*). As cyclic electron flow was first observed in vitro, there has been a long debate about whether it actually exists under physiological conditions (e.g., refs *8*−*14*) and, if so, what its function is. There is now a growing body of evidence that shows it does occur as a normal part of photosynthesis (e.g., refs *15*−*22*) and that it might be required both to balance the production of ATP and NADPH to match the requirements of carbon fixation and to generate a proton gradient to regulate light harvesting (*23*, *24*). Nevertheless, many questions concerning cyclic electron flow remain. In particular, the pathway by which electrons pass from the acceptor side of PSI back into the electron transport chain is as yet undefined. A recently discovered novel heme (*25*), in the cytochrome b_6f complex, has however been suggested as a possible intermediate (*26*). A newly identified protein, PGR5, has also been implicated in cyclic electron flow (*4*, *5*), though its function remains to be defined.

In addition to the exact electron path, the regulation of cyclic electron flow also remains unclear. The cyclic and linear pathways share a number of common carriers, from plastoquinone (PQ)[1] to ferredoxin (Fd), and thus might be in competition with one another. To rationalize the occurrence of cyclic flow, a number of models have been put forward, suggesting that the two pathways must be, to a greater or lesser extent, segregated.

(i) The restricted diffusion model is the first. It is well-known that photosynthetic complexes are unevenly distributed in the thylakoid membrane. In particular, photosystem II (PSII) is mostly located in the appressed grana stacks, while PSI is concentrated in the nonappressed membranes (the stroma lamellae, the grana margin, and the end membranes). The cyt b_6f complex is homogeneously distributed (*27*; see also ref *28*). Because of the restricted diffusion of the soluble electron carriers [PQ (*29*) or plastocyanin (*30*)], it has been proposed that PSII would be

[†] We acknowledge the UK Biotechnology and Biological Sciences Research Council for a studentship to B.N. and the Royal Society for a European exchange grant to G.N.J. and G.F. Funding by the CNRS is also acknowledged.

* To whom correspondence should be addressed: UMR 7141 CNRS, Institut de Biologie Physico-Chimique, 13 rue Pierre et Marie Curie, F-75005 Paris, France. Telephone: +33 1 5841-5101. Fax: +33 1 5841-5022. E-mail: giovanni.finazzi@ibpc.fr.

[‡] UMR-7099 CNRS.

[§] University of Manchester.

[||] UMR-7141 CNRS.

[1] Abbreviations: 2D, two-dimensional; BN-PAGE, blue native polyacrylamide gel electrophoresis; CBB, Coomassie brilliant blue; cyt, cytochrome; DCMU, 3-(3′,4′-dichlorophenyl)-1,1-dimethylurea; ECL, enhanced chemiluminescence; ESC, electrochromic signal; Fd, ferredoxin; FNR, Fd−NADP−reductase; HA, hydroxylamine; LHC, light-harvesting complex antenna; P700, primary electron donor of photosystem I; PQ, plastoquinone; PS, photosystem; TMBZ, tetramethylbenzidine.

10.1021/bi061439s CCC: $33.50
Published on Web 10/20/2006

able to fuel only cyt b_6f complexes located in the grana (*27*). Those in the nonappressed membranes would instead be reduced by PSI, leading to cyclic electron flow.

(ii) The supercomplex model is the second. It has been proposed that cyclic electron flow might occur within tightly bound PSI−cyt b_6f supercomplexes, containing stoichiometric amounts of plastocyanin and Fd (*31*, *32*). This model has been proposed to account for the fact that electrons generated at the PSI donor side during cyclic flow are not shared with the pool of soluble acceptors, but rather seem to be thermodynamically isolated from the stroma. In addition, complete segregation between the linear and cyclic chain has been invoked as a tool for maintaining "redox poising" of cyclic flow, i.e., preventing its inhibition by either over-reduction or over-oxidation of the carriers that are involved (*33*). This model clearly represents an extreme case of the preceding one, since the idea that linear and cyclic flow occur in different thylakoid domains is conserved, the domain where cyclic flow takes place being reduced to a single PSI−cyt b_6f supercomplex.

(iii) The Fd−NADP−reductase (FNR) model (*26*) is the third. FNR can be found free in the stroma (*34*) or bound to PSI (*35*) and possibly to cyt b_6f (*36*). According to this model, PSI−FNR complexes would mainly work in linear flow, since the presence of a tight ternary complex (PSI−Fd−FNR) would result in efficient reduction of $NADP^+$. On the other hand, FNR-free PSI complexes could only reduce Fd, which would then be able to diffuse into solution and feed electrons back into the cyclic pathway, possibly via FNR bound to cyt b_6f.

(iv) The competition model is the fourth. Recently, a more dynamic view of cyclic flow has been proposed (*37*), in which the efficiency of cyclic flow would depend upon the competition between cyclic and linear flow for reduced Fd. Under physiological conditions, this competition would favor linear flow, either because of its higher affinity for Fd or because of a proximity effect, the "linear" electron carriers being located closer to PSI than the cyclic ones (see also refs *38* and *39*).

Previous studies have shown that dark-adapted leaves, subjected to pre-steady-state illumination, show a maximum of cyclic flow (*32*, *40*). In such material, the Benson−Calvin cycle is largely inactive and thus illumination leads to a fast inhibition of linear flow. The very rapid cyclic flow activity measured in these conditions excludes the involvement of a NAD(P)H-plastoquinone reductase (NDH) activity. Indeed, this is present in very small amounts (*19*) and normally shows a rather slow turnover (*41*, *42*). Upon illumination, several minutes is required for the activation of the Benson−Calvin cycle and, therefore, of linear flow. Hence, one can take advantage of this temporal separation between the onset of cyclic and linear flow upon illumination to critically re-examine the mechanism of the establishment and disappearance of cyclic flow in intact leaves. To this end, we employed a combined biochemical and biophysical approach. On the basis of this analysis, we suggest that structural explanations for cyclic flow, assuming the existence of tightly bound supercomplexes between photosynthetic electron carriers, are unlikely. Conversely, we provide support for the hypothesis that the occurrence of cyclic flow is the result of a competition with linear flow, where the relative efficiency of the two processes is solely modulated by changes in the redox state of the electron transport chain. In particular, reduction of the PSI electron acceptors is necessary for the onset of cyclic flow, its rate being ultimately set by the number of reducing equivalents stored in the PSI donor pool.

EXPERIMENTAL PROCEDURES

Experiments were performed with spinach leaves bought at the local market.

Biochemical Analysis. Chloroplasts were prepared at 4 °C, in the dark from either dark-adapted or pre-illuminated leaves. Leaves were blended very briefly in ice-cold buffer [10 mM Tris (pH 8.0), 10 mM NaCl, 5 mM $MgCl_2$, and 330 mM sucrose], and the resulting suspension was filtered through eight layers of muslin. Chloroplasts were pelleted at 1500*g* for 3 min, washed three times with the same buffer, and resuspended to a final chlorophyll concentration of 4−5 mg/mL. Thylakoids were then solubilized either with Triton-X100 (0.45−1.8%, i.e., 0.6−2.4 g of detergent/g of protein) or with freshly prepared digitonin (0.75−6%, i.e., 1−8 g of detergent/g of protein), a mixture of both (0.45% Triton and 0.75% digitonin to 2% Triton and 2% digitonin), or Tween 20 (0.75−5%) in 50 mM NaCl and 50 mM imidazole (pH 8.0) for 10−60 min at room temperature or 4 °C and at a final chlorophyll concentration of 1.5 mg/mL. The supernatant was recovered after centrifugation for 5 min at 100000*g*. Coomassie 250G and aminocaproic acid were added to final concentrations of 0.5% and 50 mM, respectively, and the sample was loaded onto a 4 to 13% BN-PAGE gel with a 3.5% acrylamide stacking gel (*43*). Strips of gel were incubated in a 0.2 to 1% SDS, 3 mM dithiothreitol solution for 20 min at 23 °C and for 3 min at 45 °C before analysis in a second dimension via SDS−PAGE (12% acrylamide). Gels were then either TMBZ and silver stained or transferred onto a PVDF membrane for immunoblotting. The position of cyt b_6f was determined by the reaction of heme-bearing proteins to the ECL medium. FNR was detected using an antibody raised against the spinach enzyme (gift of G. Forti, University of Milano, Milan, Italy). For TMBZ staining and immunotransfer, BN gels were first destained in 40% methanol and 250 mM sodium acetate (pH 5.0), as Coomassie blue inhibits TMBZ staining.

Spectroscopic Measurements. Spectroscopic measurements were performed on intact leaves with a flash spectrophotometer as described previously (*32*, *40*). P700 oxidation was assessed at 705 nm (*32*). Actinic far-red illumination was provided by an LED peaking at 720 nm, filtered through three Wratten filters 55 that block wavelengths shorter than 700 nm. A signal associated with fluorescence emission (normally <5%) was subtracted from the kinetics. The maximum extent of $P700^+$ was estimated from the kinetics of P700 oxidation as described in ref *26*.

Membrane potential changes were measured under the same actinic illumination as for the measurements of the P700 redox changes. They were detected at 520−545 nm, using a white LED source (Luxeon, Lumileds) filtered through appropriate interference filters. The photodiodes were protected from actinic light by a Schott BG 39 filter. To calculate the number of electrons transferred during illumination, the absorption signal measured under continuous illumination was divided by the signal corresponding to one charge separation. This corresponds to the extent of the

membrane potential signal induced by a saturating laser flash, in samples that were treated with DCMU and hydroxylamine (HA), to inhibit PSII activity (*44*). k_{iPSI} was estimated from the initial rate of membrane potential decay upon inhibition of PSII activity (*40*). Pre-illumination was provided by green LEDs with a peak emission at 520 nm (*32*).

Fluorescence Measurements. Fluorescence was measured on intact leaves with the same apparatus that was used for spectroscopy, using green excitation light provided by LEDs. Pre-illumination and leaf excitation were performed with the same green light, and fluorescence was measured on the opposite face of the leaf. The time resolution of the method is 10−20 μs. To estimate the actinic light intensity, fluorescence-induction kinetics were measured in the presence of saturating concentrations of DCMU. We evaluate the time t at which the variable fluorescence yield was $\sim^2/_3$ of the maximum value. This provides an estimate of the incident photon flux, with a precision of ±10%. As shown in ref *32*, an average of one photon per PSII center is absorbed at time t, and the PSII photochemical rate constant, k_{iPSII}, is thus equal to $1/t$.

RESULTS

Biochemical Analysis of Thylakoid Membranes Purified from Dark-Adapted and Illuminated Spinach Leaves Does Not Reveal the Presence of PSI−cyt b_6f Supercomplexes. To test the possible involvement of tightly bound PSI−cyt b_6f supercomplexes in the onset of cyclic electron flow in C3 plants, we isolated intact chloroplasts from dark- and prolonged light-adapted leaves, i.e., under conditions where previous work has pinpointed a high and low efficiency of cyclic flow, respectively (e.g., refs *32* and *40*). They were then further analyzed biochemically in an attempt to identify possible specific PSI−cyt b_6f interactions, using the Blue Native gel system developed by Schägger and co-workers to isolate mitochondrial supercomplexes (*43*). This technique associates mild solubilization of membranes and separation of solubilized complexes using a native gel system and has successfully been used on plant material to characterize chloroplastic (*43*, *45*, *46*) and mitochondrial supercomplexes (*47*−*49*).

Membranes were solubilized with mild detergents, i.e., Triton X-100, digitonin, a mixture of both, or Tween 20. As expected, Tween 20 did not solubilize the membranes. On the other hand, 6% digitonin (8 g of digitonin/g of protein) or 1.8% Triton X-100 (2.4 g of Triton X-100/g of protein) was sufficient to solubilize most or all of the cyt b_6f and PSI, while leaving most of the PSII and LHCII in the pellet. A mixture of 0.45% Triton X-100 and 0.75% digitonin was sufficient to obtain the same result, higher concentrations resulting in the total solubilization of membranes (not shown).

Figure 1 shows the biochemical analysis of spinach membranes from dark-adapted or light-treated leaves, solubilized with 6% digitonin. In spite of functional differences in cyclic flow (*32*, *40*; see also below), the gel profiles of the two samples are very similar. Bands corresponding to high-molecular weight complexes are visible above the well-defined PSI−LHCI band. However, TMBZ and ECL staining, which are specific for heme-containing proteins and very sensitive, do not indicate the presence of cyt b_6f (Figure 1A),

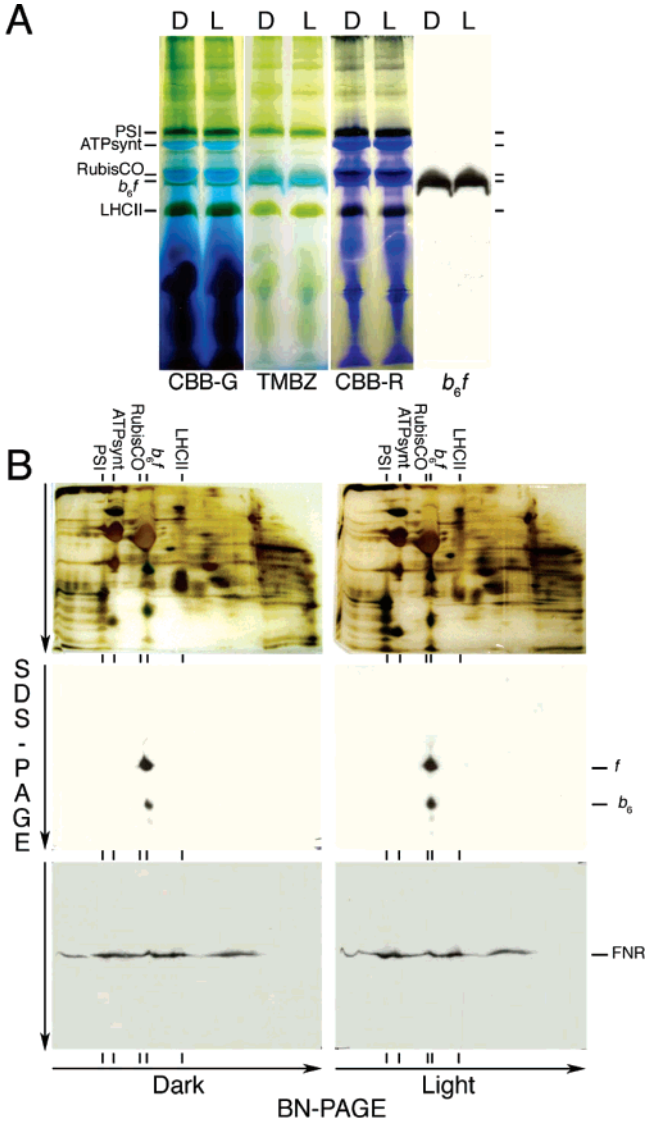

FIGURE 1: Biochemical analysis of digitonin-solubilized spinach chloroplasts, extracted from dark-adapted (D) or light-treated (L) leaves. (A) BN-PAGE (4 to 13%) after migration (CBB-G), after destaining and TMBZ staining (TMBZ), after CBB restaining (CBB-R), or after ECL revelation of heme-containing proteins (b_6f). (B) 2D BN/SDS−PAGE of the same sample, TMBZ and silver stained, or ECL revelation of heme-containing proteins (cyt f and b_6 are indicated). Cyt b_6f migrates as a dimer, and no higher-molecular weight band that would be involved in a PSI−b_6f supercomplex is observed, either via BN-PAGE or via 2D PAGE. 2D BN/SDS−PAGE gels were also immunoblotted with an antibody directed against spinach FNR. No major difference in the association of FNR with either PSI or cyt b_6f is observed in dark-adapted vs light-treated leaves. The position of the major complexes is indicated: PSI, photosystem I; ATPsynt, ATP synthase; RubisCO, ribulose bisphosphate carboxylase/oxygenase; b_6f, cytochrome b_6f complex; and LHCII, trimeric light-harvesting complex II.

which migrates as a unique band that is attributed to the dimer when compared to the migration of the purified complex. This is confirmed by the analysis of each strip in a second SDS−PAGE dimension: whereas the high-molecular weight bands contain PSI−LHCI subunits, no trace of cyt b_6f is detectable, with either TMBZ, silver staining, or immunodetection (Figure 1B). They probably correspond to PSI supercomplexes containing different amounts of LHCI and LHCII (*47*). We note that some differences can be observed in the lower-molecular weight part of the gel,

confirming that the technique is sufficiently sensitive for the detection of relatively subtle changes. Solubilization supernatants loaded onto sucrose gradients did not show PSI−cyt b_6f comigration, and the cyt b_6f migrated as a dimer (not shown). Membranes solubilized with Triton X-100 showed a slightly different BN-PAGE migration pattern, the most important difference being the presence of monomeric cyt b_6f in the Triton supernatant (not shown). No higher-molecular weight complex containing cyt b_6f was visible, either in the first BN-PAGE dimension or in the second SDS−PAGE dimension. Similar results were obtained in the Triton- and digitonin-treated samples (not shown).

The PSI−FNR Association Is Similar in Thylakoid Membranes Isolated from Dark- or Light-Adapted Leaves. As mentioned in the introductory section, a differential association of the FNR enzyme has previously been proposed to explain changes in the efficiency of cyclic electron flow between dark- and light-adapted leaves. In particular, PSI complexes with bound FNR would display an enhanced NADP reduction, leading to linear flow, while PSI complexes devoid of FNR would be limited in NADP reduction, leading to enhanced cyclic electron flow (see the introductory section). Consistent with this hypothesis, previous reports show that FNR is associated with thylakoid membranes in spinach leaves (*34*) and that membrane-bound FNR is more efficient in NADP reduction than its soluble counterpart (*50*). Biochemical and mutagenic analyses have shown that this enzyme can be bound to either cyt b_6f (*36*) or PSI (*35*), suggesting a variety of FNR partners on the thylakoid membrane.

To further investigate the binding capacity and possible dynamics of FNR relative to the occurrence of cyclic electron flow, the localization of FNR was investigated by two-dimensional BN/SDS−PAGE of solubilization supernatants of dark- and light-adapted spinach leaves. Figure 1B shows that FNR comigrates with PSI and cyt b_6f, but also with other complexes of the thylakoids. When thylakoid membranes were prepared and washed several times, the same pattern was observed (Figure 2). This indicates that the high-molecular weight forms of FNR observed in intact chloroplasts (Figure 1B) do not reflect the presence of large aggregates of this protein in its soluble form but rather indicate the existence strong and specific interactions of this protein with the membrane complexes.

In addition, no significant changes in the mode of interaction of FNR with thylakoid complexes, particularly with PSI, could be seen between samples isolated from dark-adapted and illuminated leaves (Figure 1B), suggesting that the dissociation of tightly bound PSI−FNR complexes is not an absolute prerequisite for the onset of cyclic electron flow.

Redox Changes of the PSI Acceptors and Donors Modulate the Efficiency of Cyclic Flow. The results reported above suggest that the changes in the efficiency of cyclic electron flow reported between dark-adapted and illuminated leaves do not correlate with differences in complex association in the photosynthetic membranes. On the other hand, differences in the extent of cyclic flow can be observed in different dark-adapted leaves.

Previous work has shown that when dark-adapted leaves are illuminated with low-intensity far-red light, P700 is oxidized following a biphasic kinetic, with there being a great deal of variability in the relative proportions of the fast and

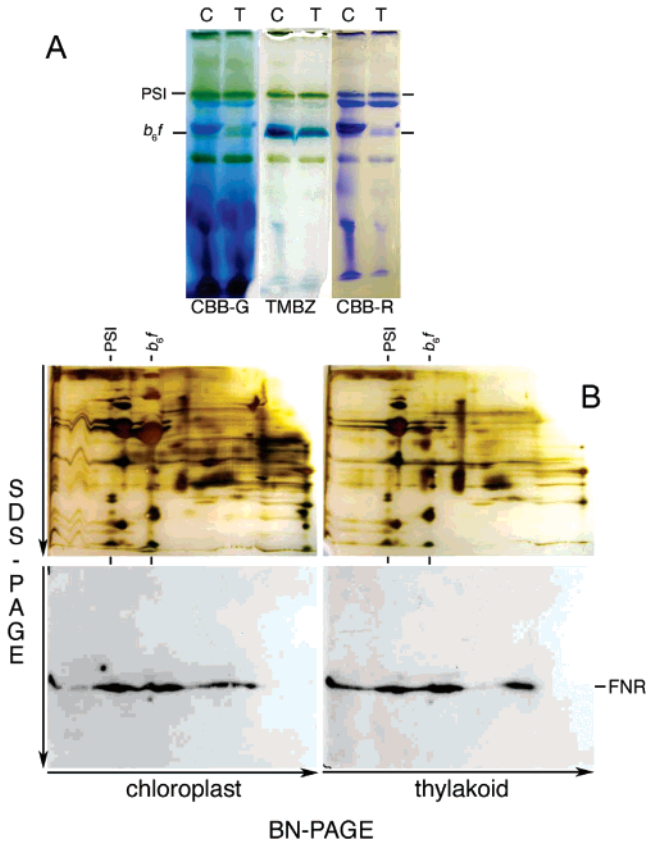

FIGURE 2: Biochemical analysis of digitonin-solubilized spinach chloroplasts (C) and thylakoids (T). (A) BN-PAGE (4 to 13%) after migration (CBB-G), after destaining and TMBZ staining (TMBZ), and after CBB restaining (CBB-R). (B) 2D BN/SDS−PAGE of TMBZ and silver stained or immunoblotted with an antibody directed against spinach FNR. No major difference in the association of the FNR with PSI or cyt b_6f is seen in chloroplasts or thylakoids, indicating strong and specific interactions of FNR with the membrane complexes.

slow phases of oxidation (*26*). This is illustrated in Figure 3, where three different leaves are compared. There, kinetics of P700 oxidation are presented upon illumination with a weak far-red light source ($k_{iPSI} = 8\ s^{-1}$) under dark-adapted (curve 1), preflashed (curve 2), and light-adapted conditions (curve 3). Clearly, P700 oxidation is biphasic in dark-adapted leaves, with large variations in the relative amplitude of the fast and slow phase, as previously reported (*26*, *37*). This biphasicity was explained by the presence of two different PSI populations (*26*). The first one, corresponding to the fast phase, is ascribed to PSI centers involved in linear electron transfer (*26*). There, P700 oxidized by the linear pathway is not re-reduced by electron transfer from PSII under far-red illumination in these centers. The second PSI population, corresponding to the slow phase, would stem from centers involved in cyclic flow. For these complexes, net P700 oxidation is slowed, because of the recycling of electrons through PSI.

The biphasicity is suppressed by a short preflash, which induces the appearance of a long lag period (~3 s) before the onset of oxidation, and also slows the overall rate of P700 oxidation, in agreement with previous results (*37*). Finally, light adaptation of the leaves for several minutes largely increases the rate of P700 oxidation, which becomes maximal while remaining largely monophasic. This raises the following question: What is the mechanism responsible

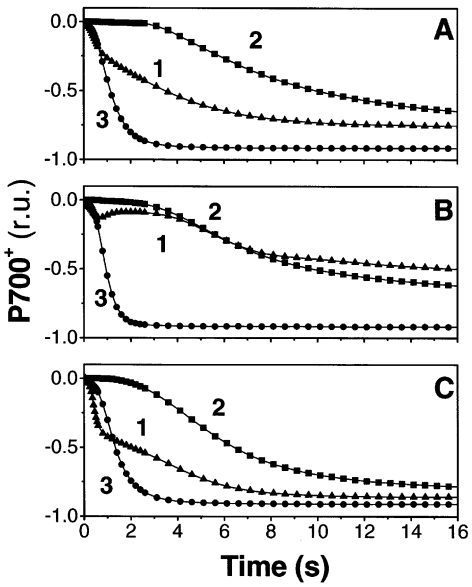

FIGURE 3: Oxidation of P700 during illumination of dark-adapted spinach leaves with far-red light. Panels A−C depict data from three different leaves, dark-adapted for more than 1 h. Curve 1 is for P700 oxidation kinetics upon illumination with far-red light ($k_{iPSI} \sim 7\ s^{-1}$). Curve 2 is for P700 oxidation kinetics in the same dark-adapted leaves, following illumination with a flash (150 ms) of green light ($k_{iPSII} \sim 830\ s^{-1}$) and dark adaptation for 5 s prior to far-red illumination. Curve 3 is for leaves that were pre-illuminated for 7 min with green light ($k_{iPSII} \sim k_{iPSI} \sim 90\ s^{-1}$) and then dark-adapted for 1 min before P700 oxidation kinetics were measured with far-red illumination.

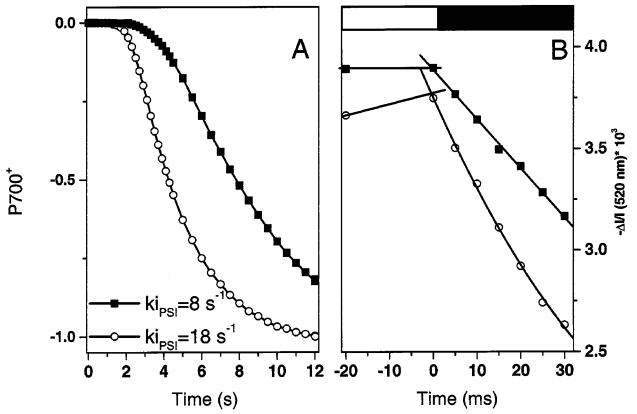

FIGURE 4: Light intensity dependence of P700 oxidation (A) and of the electrochromic signal (ECS, B) measured under far-red illumination. P700 oxidation and ECS onset were assessed in a dark-adapted leaf, which was pre-illuminated with a saturating green flash (same conditions as in Figure 3, curve 2). Two far-red intensities were used: (■) k_{iPSI} of 8 s^{-1} and (○) k_{iPSI} of 18 s^{-1}. k_{iPSI} was then measured in the same leaf as the difference between the slopes measured before and after switching the light off. The leaf was left in the dark for at least 1 h before consecutive measurements were performed. The white rectangle means the actinic light was on and the black rectangle the actinic light was off. See the text for further details.

for the slowing of P700 oxidation by the preflash? Because the Benson−Calvin cycle is inactive in dark-adapted leaves, the flash will reduce electron acceptors located downstream of PSII, including intermediates of the electron transport chain as well as stromal electron acceptors. This reduction is accompanied by the appearance of a long lag in P700 oxidation kinetics. This lag should correspond to the time taken to remove electrons from the PSI donor pool. Indeed, P700 will be the last component of the electron transport chain to be oxidized, due to its positive redox potential. However, both the lag and the deceleration of the P700 oxidation rate observed after the preflash could reflect a blockage of forward electron flow, because of the reduction of the acceptor pool (*51*). This might result in enhanced charge recombination between $P700^+$ and its reduced primary electron acceptor, leading to a deceleration of P700 oxidation kinetics.

To test this, we compared the kinetics of P700 oxidation at two different intensities of far-red light, measured under the conditions of trace 2 (i.e., short preflash). We found that the maximum rate of P700 oxidation was increased by a factor of ~2 when the light was doubled [$k_{iPSI} = 8$ and 18 s^{-1} (Figure 4A)]. This rules out any limitation of electron flow by a dark process as expected in the case of a blockage caused by over-reduction of the acceptor pool. Consistent with this, we observed a substantial photosynthetic activity under the same conditions, as evidenced by the appearance of a sustained electrochromic shift signal (ECS) of carotenoids upon far-red illumination (not shown). This signal is linearly related to the generation of a transmembrane electrochemical proton gradient (e.g., ref *52*), which is in turn related to PSI and PSII turnover. Starting from the difference between the slopes of the ECS measured immediately before and after switching off the light (Figure 4B), we were able to quantify the PSI turnover (see, e.g., refs *12* and *32*). At the end of the lag phase of P700 oxidation, (i.e., after illumination for 3 and 1.5 s), the rate of PSI turnover was measured to be 10 and 20 s^{-1} for the two intensities of the far-red illumination that were employed, in agreement with the 2-fold increase estimated from P700 oxidation kinetics.

Moreover, we estimate the total number of electrons stored in the PSI donors by computing the total number of turnovers occurring during the lag phase (e.g., 8 electrons/s × 3 s = 24 electrons). We found that this range is compatible with the full pre-reduction of the donors estimated per PSI reaction center but is too large to be explained solely on the basis of electron storage in the PQ, cyt b_6f, and plastocyanin pools. We conclude therefore that (i) neither the lag nor the deceleration of the P700 oxidation kinetics reflects a blockage in electron transport. (ii) The lag is dominated by the oxidation of PSI electron donors. However, part of this turnover exceeds the storage capacity of the chain. (iii) Recombination between $P700^+$ and its electron acceptors during the lag is rather unlikely. Indeed, the very high rate of turnover measured is not compatible with sustained recombination, which would require a non-negligible fraction of P700 to be in the oxidized state. Clearly, this is not the case during the lag, where all the P700 is reduced. Therefore, it is likely that both the appearance of the lag and the consecutive deceleration of P700 kinetics reflect the occurrence of cyclic electron flow. Furthermore, (iv) since no PSI centers are oxidized during the first seconds of far-red illumination, it appears that all PSI centers are capable of participating in cyclic electron flow in preflashed leaves.

Reduction of PSI Acceptors Triggers the Onset of Cyclic Flow around PSI. The data of Figures 3 and 4 unambiguously indicate that it is the redox state of the electron transport chain itself, rather than the supramolecular structure

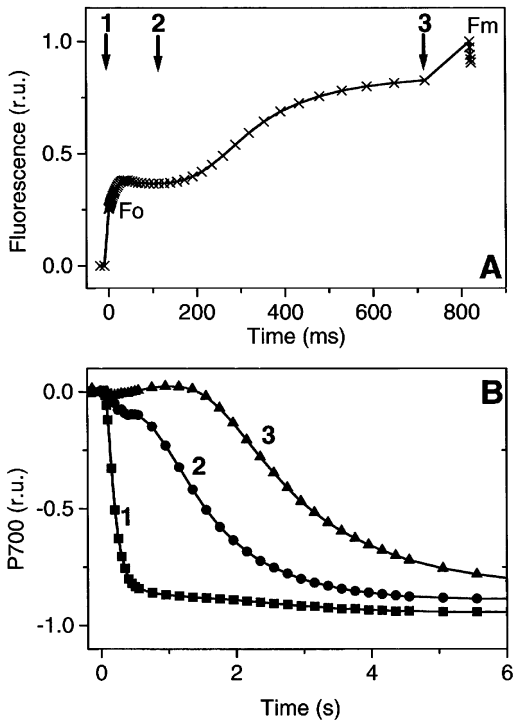

FIGURE 5: Changes in the efficiency of cyclic flow during a dark-to-light transition in spinach leaves. (A) Fluorescence induction curve under green light illumination ($k_{iPSII} \sim k_{iPSI} \sim 100\ s^{-1}$). (B) P700 oxidation kinetics as induced by far-red illumination. Trace 1 is for the dark-adapted state. Trace 2 is for the leaf that was pre-illuminated for 110 ms with the same green light as in panel A, and P700 oxidation kinetics were measured under far-red light ($k_{iPSI} \sim 7\ s^{-1}$), immediately after the green light was switched off. Trace 3 is for leaves that were pre-illuminated for 700 ms with the same green light and analyzed for P700 oxidation, as for trace 2. All traces were deconvoluted from fluorescence emission as explained in Experimental Procedures. F_o is the minimum fluorescence emission. F_m is the maximum fluorescence emission, achieved by illumination with an additional saturating pulse ($k_{iPSII} \sim 830\ s^{-1}$).

of the thylakoid membrane, which modulates the efficiency of cyclic flow. Two non-mutually exclusive hypotheses can equally account for this observation. The reduction of the PSI donors may promote cyclic flow, essentially by increasing the number of electrons available to P700, as discussed above. Alternatively, in the presence of an inactive Benson−Calvin cycle, reduction of soluble PSI acceptors (primarily $NADP^+$) may also enhance cyclic flow by preventing electron transfer from the PSI acceptor side to the linear chain and therefore increasing the number of electrons injected into the cyclic pathway. To discriminate between these two possibilities, we exploited the temporal separation in the reduction of PSI acceptors and donors, which is observed upon illumination of leaves with low light. This is shown in Figure 5A, which presents a fluorescence profile observed upon illumination of a dark-adapted leaf. The fluorescence increase reflects the progressive inhibition of PSII, resulting from the reduction of the electron acceptor, Q_A. This stems from CO_2 assimilation being inactive, which results in the progressive reduction of the electron acceptors located downstream of Q_A during illumination.

The polyphasic character of this curve witnesses the different timings for the reduction of acceptor pools located downstream of PSII. Following a first increasing phase, a plateau is observed, which can be unequivocally attributed to the reduction of the PSI acceptors, on the basis of (i) its selective suppression upon isolation of thylakoid membranes, i.e., once the soluble PSI acceptors are removed by purification (F. Rappaport and P. Joliot, unpublished results) and (ii) its disappearance in *Arabidopsis* mutants devoid of plastocyanin (*53*) and in barley plants without PSI (G. Finazzi, unpublished results). The plateau character is also consistent with this attribution, as no fluorescence increase is expected during reduction of PSI acceptors, which have no direct access to Q_A. This pool has been estimated to represent ~10 reducing equivalents (*32*). The subsequent slow increase phase corresponds to the reduction of the PQ pool, which results in progressive Q_A reduction due to direct equilibration of Q_A with PQ via the Q_B pocket of PSII (e.g., ref *54*).

Figure 5B shows measurements of P700 oxidation in a leaf subjected to the same illumination conditions as in panel A. Kinetics of P700 oxidation were measured either prior to illumination (trace 1), after illumination for 110 ms (trace 2), or after illumination for 700 ms (trace 3), which correspond to the end of the plateau and the slow increase. As described above, in the case of trace 2, the PSI soluble acceptors are mostly reduced, while the PSI donors are largely oxidized. On the other hand, both the PSI donors and acceptors are in the reduced state in the case of trace 3. Consistent with this, a very large lag in P700 oxidation was seen in trace 3 (confirming that the PQ pool was reduced; see above), while only a small lag could be detected in trace 2, indicating that this short illumination did not modify the redox state of the PQ pool when compared to the dark state. Yet, the efficiency of cyclic flow, which was close to zero in the dark-adapted leaf, was largely enhanced in trace 2. This clearly indicates that it is the redox state of PSI acceptors which mainly modulates the injection of electrons from PSI into the cyclic pathway. Note that the fast phase of P700 oxidation was not completely suppressed under this condition, suggesting that some linear flow still occurred in a small fraction of PSI complexes. Finally, the rate of cyclic flow was still slightly increased upon reduction of the PQ pool (trace 3), suggesting that the overall rate of cyclic flow is defined by the number of electrons available for PSI reduction. Note that the experiment presented in this figure refers to a leaf showing a particularly low efficiency of cyclic flow in the dark (see Figure 3). This was chosen on purpose, to illustrate the consequences of the different times of pre-illumination. However, the same effect could be reproduced in all the leaves that were tested, including those showing a better efficiency of cyclic flow in the dark (not shown).

Dark Incubation Promotes Recovery of Cyclic Electron Flow in Light-Adapted Leaves. Besides pinpointing the fundamental role of the redox state of the PSI electron acceptors in promoting the onset of cyclic flow, the data shown above also indicate that activation of CO_2 fixation by the Benson−Calvin cycle, as achieved by a prolonged pre-illumination of the leaf, is sufficient to largely suppress cyclic flow in far-red light. This inhibition is clearly reversible in the dark, as shown in Figure 6, which presents a typical time course of the recovery of cyclic electron flow upon dark adaptation of a light-treated leaf. The occurrence of cyclic flow was probed after different lengths of dark incubation after illumination for more than 10 min, by measuring P700 oxidation kinetics. Panel A shows data for

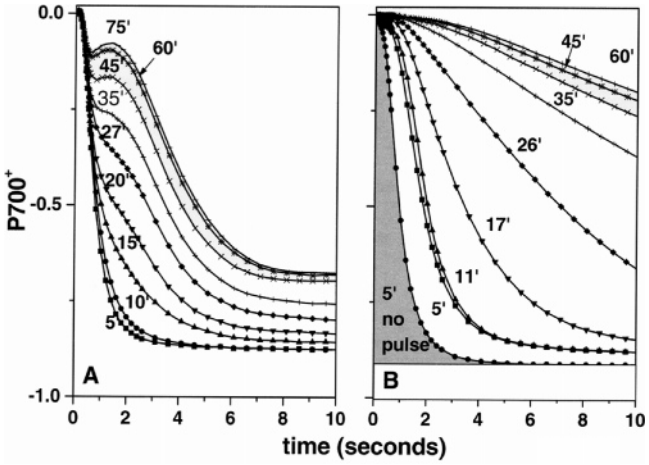

FIGURE 6: Transition from linear to cyclic flow during a light-to-dark transition. A leaf was light-adapted for more than 10 min with green light ($k_{iPSII} \sim k_{iPSI} \sim 100\ s^{-1}$). Kinetics of P700 oxidation were then measured at the indicated dark times either in the absence (A) or in the presence (B) of a short pre-illumination flash with saturating green light ($k_{iPSII} \sim 830\ s^{-1}$). The green light and the far-red illumination were separated by a dark incubation period of 5 s, as in curve 2 of Figure 3.

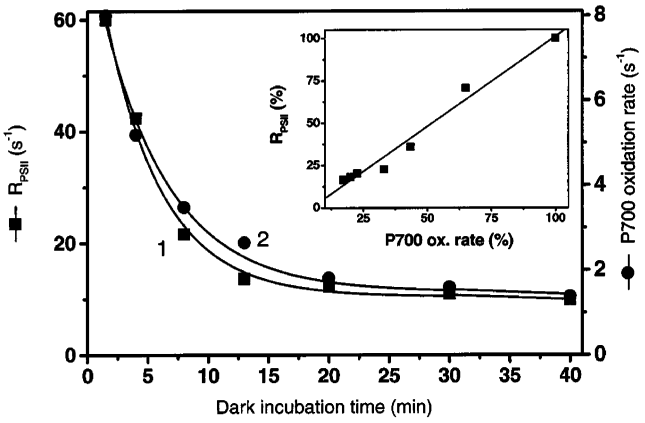

FIGURE 7: Changes in linear and cyclic electron flow rate during a light-to-dark transition. Trace 1 (■) shows changes in PSII efficiency during dark adaptation. A leaf was pre-illuminated for 8 min with actinic light ($k_{iPSII} \sim k_{iPSI} \sim 130\ s^{-1}$, trace 1). It was then left in the dark for 40 min during which time it was periodically exposed to ~1 s pulses of green light (same intensity as during the pre-illumination) followed by saturating flashes to determine F_m. The relative rate of PSII reaction (R_{PSII}) was determined according to Genty's formula: $R_{PSII} = (F_m - F_s)/F_m$ (*55*), where F_m represents the maximum fluorescence recorded during the illumination and F_s is the steady-state level of fluorescence emission during the ~1 s pulse. Trace 2 (●) shows changes in the rate of P700 oxidation during dark adaptation. The same leaf employed for fluorescence measurements was used to evaluate the P700 oxidation rate during the dark recovery. The leaf was submitted to the same pulse of green light after various periods of illumination, and the kinetics of P700 oxidation was measured with a weak far-red excitation ($k_{iPSI} = 8\ s^{-1}$) given immediately after the green source had been switched off. The inset shows the correlation between R_{PSII} and $P700^+$.

leaves where P700 oxidation kinetics were measured in the absence of the preflash. When the flash was omitted, fast, monophasic oxidation was observed during the first 5 min of dark adaptation, after which a biphasic behavior appeared. After dark adaptation for 10 min, we observe a progressive decrease in the amplitude of the fast phase. The $t_{1/2}$ of this process is ~20 min, and at steady state (darkness for ~75 min), only 10% of the fast phase remained (Figure 6A), as reported previously (*26*).

As in fully dark-adapted leaves (Figure 3), addition of a preflash prior to far-red illumination substantially affects the kinetics of P700 oxidation (Figure 6B). Immediately following actinic illumination, this flash had the effect of lengthening the short lag in the oxidation (~2 times), a phenomenon we ascribe to the reduction of the PQ pool. However, the overall shape of the oxidation curve and the maximum rate of oxidation were unaltered. For longer periods of dark adaptation (>5 min), the preflash suppressed the biphasicity otherwise seen (panel A). Instead, a monotonic oxidation curve was obtained, with an increasing lag phase and a progressive deceleration, with the $t_{1/2}$ for P700 oxidation increasing from 1 to ~20 s after dark adaptation for 1 h.

Cyclic Electron Flow Efficiency in C3 Plants Is Linked to the Assimilatory Capacity of Leaves. In a "perfect" cyclic electron flow system, electrons would be indefinitely recycled around PSI so that, in the absence of PSII activity, the redox state of P700 should rapidly reach a given value (close to 100% reduced, depending on the irradiance used) which would remain stable as long as the light is on. This is clearly not the case in our experiments, where a progressive oxidation of P700 is observed upon illumination with far-red light. This has been previously interpreted in terms of a leak of electrons from the cyclic pathway (*26*, *32*), which leads to its progressive inactivation. To understand the nature of this leak, we have compared the changes in the efficiency of cyclic flow and in the activation state of the enzymes of the Benson−Calvin cycle during a light-to-dark transition. The former parameter was evaluated from the maximum rate of P700 oxidation (Figure 7, curve 2), which is directly related to electron leak and therefore inversely related to cyclic flow. The deactivation of the CO_2 assimilatory cycle was followed by measuring chlorophyll fluorescence during the light-to-dark transition (Figure 7, curve 1). Toward this end, steady-state light-adapted leaves were transferred to darkness and then, after various time periods, exposed to actinic light for 1 s. At the end of this light period, a saturating flash of light was applied to estimate the maximum fluorescence emission, F_m. This protocol allowed an estimate of PSII efficiency (*55*), which, given that a single actinic intensity was used throughout, is proportional to the rate of PSII turnover (R_{PSII}).

As shown in Figure 7, we found a strong correlation between the decrease in the rate of cyclic electron flow leak and the rate of linear flow (Figure 7, inset), suggesting that the latter is the main cause of the leak from the cyclic pathway, as expected in the case of a simple competition between the two pathways.

DISCUSSION

Although cyclic flow has long been recognized in vitro, it is only recently that evidence that it occurs in C3 plants under normal growing conditions has begun to accumulate (e.g., refs *8* and *9* for further discussion). If photosynthetic electron transport is not, in fact, simply dominated by the linear pathway, then it is necessary to explain how electron flux is shared between the two processes. As it is recognized that a substantial part of the electron carriers (at least those embedded in the thylakoid membrane and lumen) is shared

between linear and cyclic electron flow, the two pathways are liable to compete with one another for the same electrons. Two extreme processes can be considered that might explain how linear and cyclic pathways can coexist: (i) a physical segregation of the two types of electron transport chains in different compartments, which would prevent any competition between the two systems (in this case, the proportion of linear vs cyclic would be essentially determined by the amount of PSI in each compartment) and, alternatively, (ii) the coexistence of the two electron transport chains in the same environment, where the relative efficiency of the two processes is determined by their respective kinetic efficiency (i.e., the two pathways operate in simple competition).

According to the structural models outlined in the introductory section (the "restricted diffusion", "supercomplex", and "FNR" models), limited functional interaction between cyclic and linear flow is achieved through the physical confinement of the soluble electron carriers involved in either linear or cyclic electron compartments. In particular, the supercomplex and FNR hypotheses assume that the soluble carriers involved in cyclic flow (both plastocyanin and Fd in the first case, only Fd in the latter) are thermodynamically and physically isolated from the rest of the electron transfer chain. This suggests that interactions between the different components of the PSI−cyt b_6f or PSI−FNR complexes themselves must be strong enough to prevent a fast release of the soluble electron carriers (plastocyanin or Fd) under conditions where cyclic electron flow is active but much weaker or absent (dissociation of the complexes) when linear flow prevails. Both the biochemical and biophysical analyses, however, question this hypothesis. No PSI−cyt b_6f interactions could be detected by mild solubilization, BN-PAGE analysis in either dark- or light-treated leaves, i.e., under conditions where the efficiency of cyclic flow varies to a large extent. This technique has, however, been successfully employed in isolating and characterizing fragile supramolecular membrane complexes in bioenergetics (see, e.g., refs *43*, *45*−*49*, and *56*−*60* for recent applications). In addition, no major changes in the association mode of FNR with either PSI or cyt b_6f could be identified under the same conditions. Very similar results have been obtained in plants subjected to a drought stress (not shown), i.e., a condition that largely enhances cyclic electron flow (*21*). Furthermore, we found here that all of the PSI complexes present in a leaf can operate in either linear or cyclic flow, depending on the conditions that are employed (Figures 3 and 7). This result again speaks against compartmentalization being absolutely required for the occurrence of cyclic electron flow, in agreement with recent results (*37*).

Thus, we conclude that linear and cyclic flow are not physically separated but, rather, that the two systems are in dynamic competition. The question of where this competition occurs arises. We believe that the major pathway for cyclic flow is through electron donation from Fd to cyt b_6f, at least under our experimental conditions. Indeed, the rate of turnover of cyclic flow observed here is much faster than the rates previously reported in the case of NAD(P)H-mediated electron injection into the PQ pool (e.g., refs *41* and *42*). Moreover, while differences in the cyclic electron flow rate were reported between wild-type (WT) and tobacco Ndh^- plants in anaerobiosis, no such differences were seen in aerobiosis (*20*), i.e., the conditions explored in this work. In light of this, we propose that, once a reducing equivalent is generated at the reducing side of PSI, its involvement in either linear or cyclic flow is determined at the level of the Fd pool. As the diffusion of this protein is not confined, its oxidation by FNR and the $NADP^+$ pool would lead to linear flow, while interaction with a putative Fd oxidizing site localized on the stromal side of cyt b_6f would initiate cyclic flow. The latter might be mediated by a FNR molecule bound to cyt b_6f, which we clearly identify in our samples, in agreement with previous reports (*36*).

This model is supported by the data of Figure 5. In dark-adapted leaves, the enzymes of the Benson−Calvin cycle are inactivated. CO_2 fixation is thus slow, and metabolic processes will compete poorly with cyclic flow. Under these conditions, the simple reduction of PSI soluble acceptors (primarily NADP) by a short pre-illumination is sufficient to promote a full transition of PSI complexes to the cyclic mode. After this transition, the overall rate of cyclic flow is determined by the number of electrons available for P700 turnover, i.e., by the redox state of the PSI donors. We conclude, therefore, that it is the redox state of the electron transport chain that controls the efficiency of cyclic flow, in agreement with previous findings that cyclic flow is enhanced by anaerobiosis in tobacco leaves (*20*). This control takes place at two different steps, the soluble PSI acceptors being responsible for the diversion of electrons between the linear and cyclic chains and the donors being involved in setting the overall rate of cyclic flow.

In dark-adapted leaves, cyclic flow will be maintained as long as electrons remain in the chain. This will not be indefinite, as there will always be some "leakage" from the cyclic pathway, due to residual metabolic activity and photoreduction of oxygen [the Mehler reaction (*2*)]. On the other hand, when the leaf is in a light-adapted state (Figure 6), the enzymes of the Benson−Calvin cycle are active and the latter will act as an efficient sink for electrons coming from PSI and will outcompete any cyclic electron transfer. Thus, under such circumstances, there is a rapid oxidation of P700 upon illumination with far-red light (i.e., a very efficient leakage of the cyclic pathway) even in leaves with both the PSI electron donors and acceptors reduced (Figure 3, trace 3, and Figure 6, trace 5′ no pulse). Consistent with this, a computation based on the ratio between the rates of P700 oxidation measured in light-adapted and fully dark-adapted leaves shows that the rate of P700 oxidation is ∼20 times slower under the latter condition, implying that ∼95% of the reduced acceptors formed on the acceptor side of PSI are reoxidized via the cyclic mode in the dark, while more than 80% of the electron flow becomes linear upon light adaptation.

In light-adapted leaves, the fast kinetics of P700 oxidation measured in light-adapted leaves simply reflects the time necessary to evacuate electrons already present in the electron transport chain (reduced plastocyanin, cyt *f*, Rieske, and PQ) through the PSI acceptor side. Indeed, under the weak far-red light excitation employed in these experiments, the rate of PSI photochemistry is expected to be proportional to the fraction of P700 present in its reduced (active) form. Assuming this, the area below each trace provides an estimate of the number of electrons transferred through PSI. Knowing the photochemical rate constant ($k_{iPSI} \sim 7\ s^{-1}$ in Figure 6B), we estimate that there is a turnover of 6.5 electrons per PSI

in pre-illuminated leaves (shaded area in Figure 6B). This number increases to 14 when a short saturating green flash is applied prior to far-red illumination (Figure 6B, curves 5′−11′). We attribute this difference (~7.5 electrons) to the number of reducing equivalents generated by the pulse itself and stored in the PQ pool. Nevertheless, as indicated by the fast P700 oxidation kinetics, these additional electrons are also injected into the linear path during the subsequent far-red illumination.

Previously, observations of biphasic oxidation kinetics of P700 have been explained in terms of the presence of separate "cyclic" and "linear" pools of PSI. In the context of the model presented here, however, such distinct pools are not required. Nevertheless, some heterogeneity is required in the system for us to understand the biphasic kinetics observed in the absence of pre-illumination. This might simply be explained by heterogeneity at the level of PSI electron sinks, with more and less efficient electron acceptors giving rise to heterogeneous withdrawal of electrons from P700 during illumination. However, the existence of heterogeneity at the level of PSI secondary donors cannot be excluded. It has been proposed that thermodynamically isolated compartments exist within the thylakoids (*29*), having different stoichiometries between secondary donors and P700. Again, electron transfer from PSI to its secondary acceptors may lead to fast P700 oxidation in compartments with a low secondary donor/PSI ratio, while electron recycling in the cyclic path would lead to a concomitant slow P700 oxidation in the compartments with a high secondary donor/PSI ratio. This would ultimately result in biphasic oxidation kinetics, as seen in Figure 5A, and also account for the observation of a very small fraction of PSI involved in linear turnover under conditions where the PSI acceptors, but not the donors, were reduced. This would stem from the compartments where the number of donors is so small that PSI oxidation cannot be avoided when its donors are oxidized. In any case, application of a saturating flash, which would reduce all the PSI donors and acceptors, would mask this heterogeneity, resulting in monotone kinetics.

The importance of the Benson−Calvin cycle as the main sink for electrons in competition with cyclic flow is emphasized in Figure 7, where it is shown that there is a strong correlation between the rate of leakage of electrons from the cyclic pathway and the activity of CO_2 fixation, as assayed by measurements of PSII efficiency. The model presented here assumes that, when fully active, electron flow to the Benson−Calvin cycle will efficiently outcompete the cyclic pathway. This competition is, however, carefully balanced as any change in CO_2 fixation during dark adaptation leads to a corresponding modification of cyclic flow (Figure 7). In dark-adapted leaves, reduction of FNR is likely to be the committed step in linear electron flow. If this is the case, the redox state and activity (especially related to membrane binding) of FNR are liable to be crucial in determining the fate of electrons from PSI. However, the situation under conditions of steady-state actinic illumination may in principle be different. In particular, under high-light conditions, linear and cyclic flows are liable to be in competition at the PSI acceptor side, but also at the point where electrons are re-injected into the PQ pool (e.g., refs *4*, *5*, and *20*). Typically, the rate of cyclic flow has been reported to increase under high light conditions (*37*) and under drought conditions (*21*). In these cases, kinetic control by the rate of PQ oxidation at the lumenal side of cyt b_6f might be more important than redox control by FNR in modulating linear and cyclic flows. However, even under these conditions, the electron transport chain (P700, cyt *f*, and plastocyanin) remains largely oxidized, indicating that kinetic limitation of electron flow at the level of the Rieske Fe−S center is taking place. However, as this process is a common step to both the linear and cyclic path, we do not expect the relative efficiency of cyclic and linear flow to be limited by this bottleneck kinetic step. Rather, it is likely that the relative efficiency of linear and cyclic flow may be governed by the probability of electron diversion at the stromal side of PSI also under steady-state illumination conditions. This being the case, any limitation of assimilation of CO_2 by ATP should be mirrored by overaccumulation of NDPH. By triggering cyclic flow, this should provide in turn "extra" ATP, therefore allowing linear flow to restart. In conclusion, redox modulation of cyclic flow appears to represent the simplest and most economical tool for keeping the ATP and NADPH balance during active photosynthesis.

ACKNOWLEDGMENT

We acknowledge Anne Joliot for fruitful discussions and Giorgio Forti for providing the antibody raised against spinach FNR.

REFERENCES

1. Allen, J. F. (2002) Photosynthesis of ATP-Electrons, Proton Pumps, Rotors, and Poise, *Cell 110*, 273−276.
2. Ort, D. R., and Baker, N. R. (2002) A photoprotective role for O_2 as an alternative electron sink in photosynthesis? *Curr. Opin. Plant Biol. 5*, 193−198.
3. Scheibe, R. (1987) NADP-malate dehydrogenase in C3 plants: Regulation and role of a light-activated enzyme. *Physiol. Plant. 71*, 393−400.
4. Munekage, Y., Hojo, M., Meurer, J., Endo, T., Tasaka, M., and Shikanai, T. (2002) PGR5 is involved in cyclic electron flow around photosystem I and is essential for photoprotection in *Arabidopsis*, *Cell 110*, 361−371.
5. Munekage, Y., Hashimoto, M., Miyake, C., Tomizawa, K., Endo, T., Tasaka, M., and Shikanai, T. (2004) Cyclic electron flow around photosystem I is essential for photosynthesis, *Nature 429*, 579−582.
6. Arnon, D. I., Allen, M. B., and Whatley, F. R. (1954) Photosynthesis by isolated chloroplasts, *Nature 174*, 394−396.
7. Bendall, D. S., and Manasse, R. S. (1995) Cyclic Photophosphorylation and Electron-Transport, *Biochim. Biophys. Acta 1229*, 23−38.
8. Johnson, G. N. (2005) Cyclic electron transport in C3 plants: Fact or artefact? *J. Exp. Bot. 56*, 407−516.
9. Cruz, J. A., Avenson, T. J., Kanazawa, A., Takizawa, K., Edwards, G. E., and Kramer, D. M. (2005) Plasticity in light reactions of photosynthesis for energy production and photoprotection, *J. Exp. Bot. 56*, 395−406.
10. Harbinson, J., Genty, B., and Baker, N. R. (1989) Relationship Between the Quantum Efficiencies of Photosystem-I and Photosystem-II in Pea Leaves, *Plant Physiol. 90*, 1029−1034.
11. Fork, D. C., and Herbert, S. K. (1993) Electron-Transport and Photophosphorylation by Photosystem-I in-Vivo in Plants and Cyanobacteria, *Photosynth. Res. 36*, 149−168.
12. Sacksteder, C. A., and Kramer, D. M. (2000) Dark-interval relaxation kinetics (DIRK) of absorbance changes as a quantitative probe of steady-state electron transfer, *Photosynth. Res. 66*, 145−158.
13. Laisk, A., Eichelmann, H., Oja, V., and Peterson, R. B. (2005) Control of cytochrome b_6f at low and high light intensity and cyclic electron transport in leaves, *Biochim. Biophys. Acta 1708*, 79−90.

14. Heber, U., Neimanis, S., Siebke, K., Schönknecht, G., and Katona, E. (1992) Coupled cyclic electron transport in intact chloroplasts and leaves of C_3 plants: Does it exist? If so, what is its function? *Photosynth. Res. 46*, 269−275.
15. Clarke, J. E., and Johnson, G. N. (2001) In vivo temperature dependence of cyclic and pseudocyclic electron transport in barley, *Planta 212*, 808−816.
16. Gerst, U., Schreiber, U., Neimanis, S., and Heber, U. (1995) Photosystem I-dependent cyclic electron flow contributes to the control of photosystem II in leaves when stomata close under water stress, in *Photosynthesis: From Light to Biosphere* (Mathis, P., Ed.) Vol. II, pp 835−838, Kluwer Academic Publishers, Dordrecht, The Netherlands.
17. Harbinson, J., and Foyer, C. H. (1991) Relationships between the Efficiencies of Photosystem-I and Photosystem-Ii and Stromal Redox State in Co_2-Free Air: Evidence for Cyclic Electron Flow *In vivo*, *Plant Physiol. 97*, 41−49.
18. Egorova, E. A., and Bukhov, N. G. (2002) Effect of elevated temperatures on the activity of alternative pathways of photosynthetic electron transport in intact barley and maize leaves, *Russ. J. Plant Physiol. 49*, 575−584.
19. Sazanov, L. A., Burrows, P. A., and Nixon, P. J. (1998) The chloroplast Ndh complex mediates the dark reduction of the plastoquinone pool in response to heat stress in tobacco leaves, *FEBS Lett. 429*, 115−118.
20. Joet, T., Cournac, L., Peltier, G., and Havaux, M. (2002) Cyclic electron flow around photosystem I in C-3 plants. *In vivo* control by the redox state of chloroplasts and involvement of the NADH-dehydrogenase complex, *Plant Physiol. 128*, 760−769.
21. Golding, A. J., and Johnson, G. N. (2003) Down regulation of linear and activation of cyclic electron transport during drought, *Planta 218*, 107−114.
22. Miyake, C., Miyata, M., Shinzaki, Y., and Tomizawa, K. (2005) CO_2 response of cyclic electron flow around PSI (CEF-PSI) in tobacco leaves: Relative electron fluxes through PSI and PSII determine the magnitude of non-photochemical quenching (NPQ) of Chl fluorescence, *Plant Cell Physiol. 46*, 629−637.
23. Katona, E., Neimanis, S., Schonknecht, G., and Heber, U. (1992) Photosystem I-Dependent Cyclic Electron-Transport Is Important in Controlling Photosystem-II Activity in Leaves Under Conditions of Water-Stress, *Photosynth. Res. 34*, 449−464.
24. Cornic, G., Bukhov, N. G., Wiese, C., Bligny, R., and Heber, U. (2000) Flexible coupling between light-dependent electron and vectorial proton transport in illuminated leaves of C-3 plants. Role of photosystem I-dependent proton pumping, *Planta 210*, 468−477.
25. Stroebel, D., Choquet, Y., Popot, J.-L., and Picot, D. (2003) An atypical haem in the cytochrome b_6f complex, *Nature 426*, 413−418.
26. Joliot, P., and Joliot, A. (2005) Quantification of cyclic and linear flows in plants, *Proc. Natl. Acad. Sci. U.S.A. 102*, 4913−4918.
27. Albertsson, P. Å. (2001) A quantitative model of the domain structure of the photosynthetic membrane, *Trends Plant Sci. 6*, 349−354.
28. Dekker, J. P., and Boekema, E. J. (2005) Supramolecular organization of thylakoid membrane proteins in green plants, *Biochim. Biophys. Acta 1706*, 12−39.
29. Lavergne, J., and Joliot, P. (1991) Restricted diffusion in photosynthetic membranes, *Trends Biochem. Sci. 16*, 129−134.
30. Kirchhoff, H., Schottler, M. A., Maurer, J., and Weis, E. (2004) Plastocyanin redox kinetics in spinach chloroplasts: Evidence for disequilibrium in the high potential chain, *Biochim. Biophys. Acta 1659*, 63−72.
31. Laisk, A. (1993) Mathematical modelling of free-pool and channelled electron transport in photosynthesis: Evidence for a functional supercomplex around photosystem, *Proc. R. Soc. London, Ser. B 251*, 243−251.
32. Joliot, P., and Joliot, A. (2002) Cyclic electron transport in plant leaf, *Proc. Natl. Acad. Sci. U.S.A. 99*, 10209−10214.
33. Allen, J. F. (1983) Regulation of photosynthetic phosphorylation, *CRC Crit. Rev. Plant Sci. 1*, 1−22.
34. Forti, G., Cappelletti, A., Nobili, R. L., Garlaschi, F. M., Gerola, P. D., and Jennings, R. C. (1983) Interaction of ferredoxin and ferredoxin-NADP reductase with thylakoids, *Arch. Biochem. Biophys. 221*, 507−513.
35. Scheller, H. V., Jensen, P. E., Haldrup, A., Lunde, C., and Knoetzel, J. (2001) Role of subunits in eukaryotic photosystem I, *Biochim. Biophys. Acta 1507*, 41−60.
36. Zhang, H., Whitelegge, J. P., and Cramer, W. A. (2001) Ferredoxin:$NADP^+$ oxidoreductase is a subunit of the chloroplast cytochrome b_6f complex, *J. Biol. Chem. 276*, 38159−38165.
37. Joliot, P., and Joliot, A. (2006) Cyclic electron flow in C3 plants, *Biochim. Biophys. Acta 1757*, 362−368.
38. Heber, U., Egneus, H., Hanck, U., Jensen, M., and Köster, S. (1978) Regulation of photosynthetic electron transport and photophosphorylation in intact chloroplasts and leaves of *Spinacia oleracea*, *Planta 143*, 41−49.
39. Ziem-hanck, U., and Heber, U. (1980) Oxygen requirement of photosynthetic CO_2 assimilation, *Biochim. Biophys. Acta 591*, 266−274.
40. Joliot, P., Béal, D., and Joliot, A. (2004) Cyclic electron flow under saturating excitation of dark-adapted *Arabidopsis* leaves, *Biochim. Biophys. Acta 1656*, 166−176.
41. Burrows, P. A., Sazanov, L. A., Svab, Z., Maliga, P., and Nixon, P. J. (1998) Identification of a functional respiratory complex in chloroplasts through analysis of tobacco mutants containing disrupted plastid ndh genes, *EMBO J. 17*, 868−876.
42. Corneille, S., Cournac, L., Guedeney, G., Havaux, M., and Peltier, G. (1998) Reduction of the plastoquinone pool by exogenous NADH and NADPH in higher plant chloroplasts. Characterization of a NAD(P)H-plastoquinone oxidoreductase activity, *Biochim. Biophys. Acta 1363*, 59−69.
43. Schägger, H. (2001) Blue-Native Gels to Isolate Protein Complexes from Mitochondria, in *Mitochondria* (Pon, L., Ed.) *Methods in Cell Biology*, Vol. 65, pp 231-44 Elsevier Science BV, Amsterdam.
44. Bennoun, P. (1970) Réoxydation du quencher de fluorescence "Q" en présence de 3-(3,4-dichlorophényl)-1,1-diméthylurée, *Biochim. Biophys. Acta 216*, 357−363.
45. Thidholm, E., Lindstrom, V., Tissier, C., Robinson, C., Schroder, W. P., and Funk, C. (2002) Novel approach reveals localisation and assembly pathway of the PsbS and PsbW proteins into the photosystem II dimer, *FEBS Lett. 513*, 217−222.
46. Suorsa, M., Regel, R. E., Paakkarinen, V., Battchikova, N., Herrmann, R. G., and Aro, E. M. (2004) Protein assembly of photosystem II and accumulation of subcomplexes in the absence of low molecular mass subunits PsbL and PsbJ, *Eur. J. Biochem. 271*, 96−107.
47. Heinemeyer, J., Eubel, H., Wehmhoner, D., Jansch, L., and Braun, H. P. (2004) Proteomic approach to characterize the supramolecular organization of photosystems in higher plants, *Phytochemistry 65*, 1683−1692.
48. Krause, F., Reifschneider, N. H., Vocke, D., Seelert, H., Rexroth, S., and Dencher, N. A. (2004) "Respirasome"-like supercomplexes in green leaf mitochondria of spinach, *J. Biol. Chem. 279*, 48369−48375.
49. Eubel, H., Heinemeyer, J., Sunderhaus, S., and Braun, H. P. (2004) Respiratory chain supercomplexes in plant mitochondria, *Plant Physiol. Biochem. 42*, 937−942.
50. Forti, G., and Bracale, M. (1984) Ferredoxin-ferredoxin NADP reductase interaction. Catalytic differences between the soluble and the thylakoid-bound complex, *FEBS Lett. 166*, 81−84.
51. Siebke, K., Laisk, A., Neimanis, S., and Heber, U. (1991) Regulation of chloroplast metabolism in leaves. Evidence that NADP-dependent glyceraldehydephosphate dehydrogenase, but not ferredoxin-NADP reducatase, controls electron flow to phosphoglyceratee in the dark-light transition, *Planta 185*, 337−343.
52. Junge, W., and Witt, H. T. (1968) On the ion transport system of photosynthesis: Investigations on a molecular level, *Z. Naturforsch. 23b*, 244−254.
53. Weigel, M., Varotto, C., Pesaresi, P., Finazzi, G., Rappaport, F., Salamini, F., and Leister, D. (2003) Plastocyanin is indispensable for photosynthetic electron flow in *Arabidopsis thaliana*, *J. Biol. Chem. 278*, 31286−31289.
54. Diner, B. A. (1977) Dependence of the deactivation reactions of photosystem II on the redox state of the plastoquinone pool varied under anaerobic conditions. Equilibria on the acceptor side of photosystem II, *Biochim. Biophys. Acta 460*, 247−258.
55. Genty, B., Harbinson, J., Briantais, J.-M., and Baker, N. R. (1990) The relationship between non-photochemical quenching of chlorophyll fluorescence and the rate of photosystem 2 photochemistry in leaves, *Photosynth. Res. 25*, 249−257.
56. Stroh, A., Anderka, O., Pfeiffer, K., Yagi, T., Finel, M., Ludwig, B., and Schagger, H. (2004) Assembly of respiratory complexes I, III, and IV into NADH oxidase supercomplex stabilizes complex I in *Paracoccus denitrificans*, *J. Biol. Chem. 279*, 5000−5007.

57. Schägger, H. (2002) Respiratory chain supercomplexes of mitochondria and bacteria, *Biochim. Biophys. Acta 1555*, 154−159.
58. Schägger, H., de Coo, R., Bauer, M. F., Hofmann, S., Godinot, C., and Brandt, U. (2004) Significance of respirasomes for the assembly/stability of human respiratory chain complex I, *J. Biol. Chem. 279*, 36349−36353.
59. Dudkina, N. V., Eubel, H., Keegstra, W., Boekema, E. J., and Braun, H. P. (2005) Structure of a mitochondrial supercomplex formed by respiratory-chain complexes I and III, *Proc. Natl. Acad. Sci. U.S.A. 102*, 3225−3229.
60. Schägger, H., and Pfeiffer, K. (2000) Supercomplexes in the respiratory chains of yeast and mammalian mitochondria, *EMBO J. 19*, 1777−1783.

BI061439S